

Effective Electron Bernstein Wave Heating by Polarization Adjustment of Incident Microwave for Non-inductive Formation of Spherical Tokamak in LATE

Y. Nozawa, R. Kajita, M. Uchida, H. Tanaka, T. Maekawa

Graduate School of Energy Science, Kyoto University, Kyoto, Japan

Electron cyclotron heating and current drive (ECH/ECCD) using electron Bernstein wave (EBW) receive much attention because of no density limit, particularly on high β devices such as spherical tokamaks (STs) [1-3]. In order to use EBW for ECH/ECCD in ST devices, electron cyclotron wave (ECW) should be injected from low field side for mode conversion (MC) at the upper hybrid resonance (UHR) layer because MC via injection from high field side is not usable when the density of plasma core is higher than twice the plasma cutoff density. O-X-B and X-B methods are well-known as efficient MC methods on ECW injection from low field side. At normalized magnetic field strength $\Omega_e/\omega \sim 0.6$ (Ω_e is electron cyclotron frequency and ω is wave frequency), the former method is effective when the scale length of the density gradient (L_n) near the plasma cutoff (PC) layer is longer than half of the free space wavelength (λ_0). The latter method is effective when the L_n is between $0.1\lambda_0$ and $0.2\lambda_0$. In the intermediate region of the density gradient $0.2 < L_n/\lambda_0 < 0.5$, the MC rate is improved by adjusting the polarization and the parallel refractive index (N_{\parallel}) of the incident ECW as shown by the linear MC rate theory with cold plasma resonance absorption model in a slab geometry [4]. In this paper, we report experimental results on polarization adjustment of incident microwave for non-inductive formation of ST at the $L_n/\lambda_0 \sim 0.47$, $\Omega_e/\omega \sim 0.58$ and $N_{\parallel} \sim 0.52$ in the low aspect ratio torus experiment (LATE) device.

LATE is a small toroidal device without a central solenoid. The vacuum vessel is cylindrical, whose height is 1 m and diameter is 1 m. LATE has three 2.45 GHz magnetrons, which can generate microwave of 20 kW, respectively. TE₁₀ wave generated from the magnetron propagates in the standard rectangular waveguides. TE₁₀ wave is transferred into circular TE₁₁ wave by a rectangular-circular converter. The linear polarization of TE₁₁ wave is converted to arbitrary elliptical one by the circular waveguide polarizer [5]. The polarization of incident microwave is changeable shot by shot. The microwave is launched to the plasma from the open end of a circular waveguide on the mid-plane as shown in Figure 1(a). The

injection angle of the launcher is 68° obliquely fixed to the toroidal field (B_T). Figure 1(b) shows three types of left-handed elliptical polarizations from O-mode like to X-mode like (L1, L2 and L3). These are used in the experiments.

Figures 2(a)~(h) show four discharge waveforms where the $B_T = 72.0$ mT at $R = 0.25$ m so that the fundamental (1st) ECR layer is located at $R = 0.206$ m and the 2nd ECR layer is located at $R = 0.411$ m near the outer wall. The target plasma (gray line) is formed by the left-handed circular polarized microwave injected from the 2R port. The plasma current I_p is ramped up to 5.9 kA as the vertical field B_v and microwave power are increased up to 6.4 mT and 15 kW, respectively. When the additional microwave power of totaled 24 kW is injected from the 4R and 8R ports with the elliptical polarization, L1 (green line) or L2 (red line) or L3 (blue line) to the target plasma from 140 ms to 250 ms, the radial position of plasma current center R_p is kept at $R = 0.25$ m in each discharge by controlling B_v during the flat-top of discharges as 9.9 mT, 9.9 mT and 9.5 mT, respectively. Consequently, I_p increases up to almost the same value of 8.4 kA during the flat-top with L1 or L2 or L3. The radial locations of last closed flux surface (LCFS) on the mid-plane and the magnetic axis are at $R_{LCFS} = 0.31$ m and $R_{axis} = 0.22$ m respectively, as shown in Figure 3(a).

Figure 3(b) shows the radial density

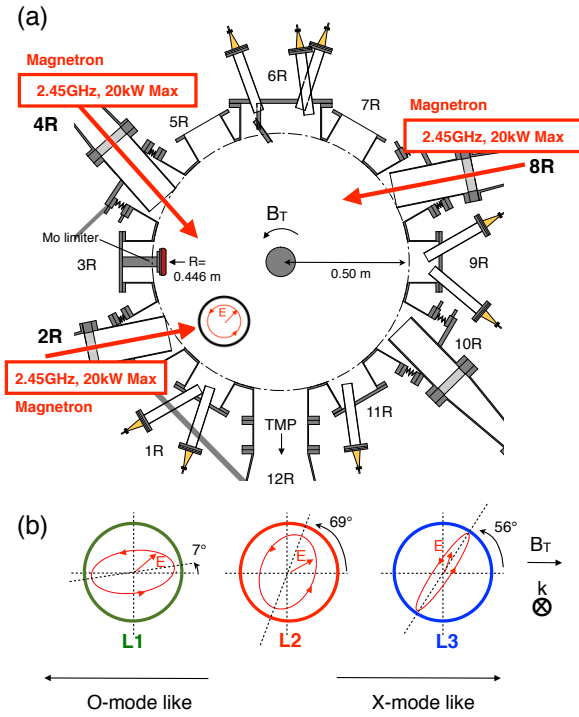


Figure 1. (a) Topview of LATE device, (b) three left-handed elliptical polarizations (L1, L2 and L3) used in the experiments.

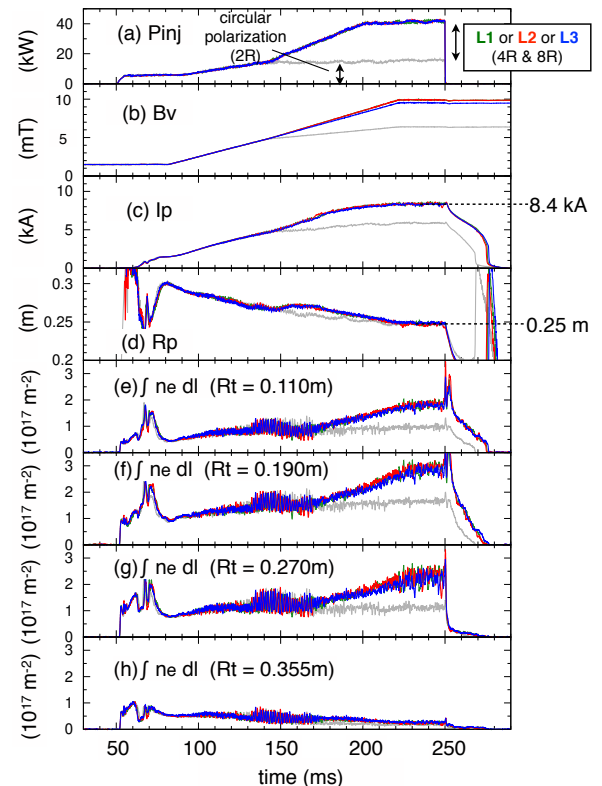


Figure 2. (a)-(h) Three discharge waveforms with L1 (green line) or L2 (red line) or L3 (blue line) and one discharge waveform of the target plasma (gray line).

profiles on the mid-plane reconstructed by using the Abel-inversion method for the cubic spline fitting curve to the four line-integrated density data (tangency radii of $R_T = 0.110$ m, 0.190 m, 0.270 m and 0.355 m, Figure 2(e)-(h)) with 30 ms time-averaging from $t = 220$ ms to 250 ms and the additional zero point at the $R_T = 0.446$ m where the radial Mo limiter is located. The differential coefficient of spline curve in $0.355 \text{ m} \leq R \leq 0.446$ m is tuned so that the value does not become negative. The density profiles outside LCFS are almost the same among three discharges. The PC and the UHR layers are located at $R = 0.36$ m and 0.37 m, respectively, between the 1st and 2nd ECR layers. The density gradient is estimated from the straight line connecting the PC and UHR layers. The normalized factors for calculation of the MC rate at the PC layer are $L_n/\lambda_0 = 0.47$, $N_{||} = 0.52$ and $\Omega_e/\omega = 0.58$. The MC rates calculated by using the linear MC theory [4] for L1, L2 and L3 are 82 %, 91 % and 64 %, respectively. The density inside LCFS is much higher than the PC density and the density peaks are located at $R = 0.26$ m between the Rax and R_{LCFS} in three discharges. The peak values for L1, L2 and L3 are $7.3 \times 10^{17} \text{ m}^{-3}$, $7.3 \times 10^{17} \text{ m}^{-3}$ and $6.7 \times 10^{17} \text{ m}^{-3}$, respectively.

Figure 3(c) shows the radial profiles of extremely ultra-violet radiation (XUV) intensity on the mid-plane. These are reconstructed by using Abel-inversion method for the spline fitting curves to line-integrated signals of seven detectors (0.164 m $\leq R_T \leq 0.322$ m). The peak positions are located

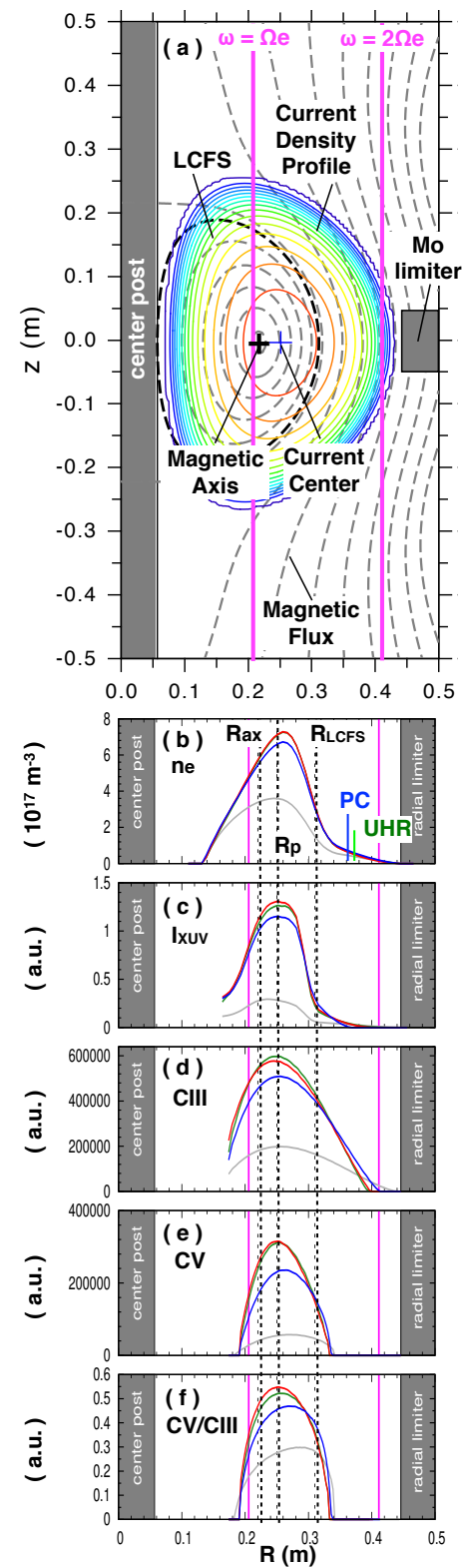


Figure 3. (a) Plasma current density and magnetic flux distributions at $t = 240$ ms, (b, c) radial density and XUV profiles on the mid-plane during the flat-top, (d-f) radial profiles of impurity line intensity (CIII, CV) and ratio CV/CIII on $z = 5$ cm during the flat-top.

at $R = 0.25$ m between the R_{ax} and R_{LCFS} . It is almost the same as R_p . These results show that EBW power is deposited near $R = 0.25$ m apart from the 1st ECR layer ($R = 0.206$ m). The peak values for L1, L2 and L3 are 1.27, 1.31 and 1.15, respectively. Figures 3(d) and (e) show the radial profiles of impurity line intensity of CIII ($\lambda = 229$ nm) and CV ($\lambda = 227$ nm) at $z = 5$ cm. Excitation energies of CIII and CV are 18 eV and 304 eV, respectively. These profiles are reconstructed by using Abel-inversion method for the third degree polynomial fitting curves to line-integrated signals ($0.174 \text{ m} \leq R_T \leq 0.320 \text{ m}$). The profiles of CIII expand outside LCFS and those of CV mainly distribute between the 1st ECR layer and R_{LCFS} . Figure 3(f) shows the CV/CIII profiles. The peak values for L1, L2 and L3 are 0.52, 0.55 and 0.47, respectively. This suggests that the electron temperature near the peak point become higher in order of $L2 > L1 > L3$. The peak values of XUV at $R = 0.25$ m for three polarizations are in order of $L2 > L1 > L3$. Therefore, the plasma core resion near $R = 0.25$ m is effectively heated by EBW when the polarization of incident microwave is L2, which is predicted by the linear MC rate theory in these experimental conditions.

Acknowledgements

This work was supported by JSPS Grant-in-Aid for Scientific Research (A) 26249142, (A) 18H03689 and (B) 18H01198.

References

- [1] V.F. Shevchenko, *et al.*, Nucl. Fusion **50**, 022004 (2010)
- [2] M. Uchida, *et al.*, Phys. Rev. Lett. **104**, 065001 (2010)
- [3] H. Tanaka, *et al.*, Fusion Energy Conf. 2016, IAEA-CN-234/EX/P4-45.
- [4] H. Igami, *et al.*, Plasma Phys. Control. Fusion **48**, 573 (2006)
- [5] Y. Noguchi, *et al.*, Plasma Phys. Control. Fusion **55**, 125005 (2013)